An induction-aware parameterization for wind farms in the WRF mesoscale model

An induction-aware parameterization for wind farms in the WRF mesoscale model

ML Mayol[1,2], GP Navarro Diaz[1,2], AC Saulo[1,3] and AD Otero[4,2]

[1] College of Sciences, University of Buenos Aires,Av. Güiraldes 2160, C1428EGA, Buenos Aires, Argentina.
[2] Computational Simulation Center, CSC - CONICET, Godoy Cruz 2390, C1425FQD, Buenos Aires, Argentina.
[3] National Weather Service, SMN, Av. Dorrego 4019, C1425GBE, Buenos Aires, Argentina.
[4] College of Engineering, University of Buenos Aires, Av. Paseo Colón 850, C1063ACV, Buenos Aires,Argentina.

E-mail: mlmayol@csc.conicet.gov.ar, alejandro.otero@csc.conicet.gov.ar

Abstract. With the aim of assessing the potential impacts of wind farms on weather and regional climate, in this work an induction-aware modified version of the Wind Farm Parameterization implemented in the WRF model is presented. It uses the undisturbed wind speed, instead of the grid cell velocity, as reference to compute the corresponding momentum sink, source of TKE and power output. The relation between the reference and grid velocity is obtained from a previous calibration process. The modified parameterization is verified by simulating one single wind turbine, showing that the power output becomes independent of the selected horizontal resolution. Finally, the performance of the new parameterization is tested over an utility-scale wind farm. It is applied to compute the wind farm efficiency for different wind directions, under several resolutions and its results compared with former parameterizations.

1. Introduction

Nowadays, as the wind farms tend to greater extensions and turbines to greater swept areas, better understanding and more accurate representation of the interaction between the wind farms and the atmospheric boundary layer (ABL) is needed. Regarding wind power forecast models, most of them do not consider the presence of turbines on the meteorological model. However, turbulent wakes produced by wind turbines can significantly impact the flow dynamics within wind farms and downstream of them. Regions of low speeds immediately behind the turbines can raise the level of turbulence over considerable distances. In large and meso scale atmospheric models, working with coarse spatial resolution which prevents a highly detailed representation of the turbines, the influence of wind turbines on the ABL, and viceversa, must be parameterized.

At global scales, wind farms have been represented, usually, through enlarged surface aerodynamic roughness length ([1], [2]). However, in this implicit parameterization approach the main wind speed deficit is represented near the surface [3], while the actual affect takes place at the hub height.

At the opposite side of the scale range, computational fluid dynamics simulations based on the large-eddy simulation (LES) method can describe the details of the fluid–structure interactions

occurring in the wind farms and resolve fine scale wake structures. These methods have been used to study the impact of wind farm wakes ([4], [5]). Despite the fact that LES is more realistic in simulating the interaction between individual wind turbines and the ABL, such degree of detail due to the spatial and temporal high resolution, is achieved at a great computational cost. Therefore it is too expensive to model a large wind farm and its consequent impact far downstream ([6]).

At regional scales one common approach is to parameterize the wind farms as an elevated momentum sink and a source of turbulent kinetic energy (TKE), as presented in [7], [8] and [9], among others. In those models the perturbed grid cell velocity (spatially averaged over a grid cell) is used to compute the forces and TKE produced by the turbines [10]. The same procedure is followed also to estimate power production. As stated in [8], it is unclear how the average wind speed within a grid cell correlates with the "undisturbed" wind speed (upwind speed at hub height) at each single wind turbine (WT) location, which is relevant for the total power output of the farm.

This work aims to address the issue of the uncertainty stated above, introducing a modified version of the Fitch's parameterization [9] where the grid cell velocity is correlated with the "reference" or "undisturbed" velocity as a function of the grid resolution. This modified wind farm parameterization is first tested through single wind turbine simulations, for different undisturbed wind speeds. Then, in order to explore the performance of this modified parameterization, the power efficiency for different wind directions in an idealized version of an utility-scale wind farm in Patagonia, Argentina, is analyzed.

2. Methodology

2.1. WRF model. Wind Farm Parameterization

The Weather Research and Forecasting Model (WRF) [11] is a state-of-the-art mesoscale atmospheric modeling system that has been extensively used for both meteorological research and numerical weather prediction. It is distributed with a wind farm parameterization (WFP) where WTs in each cell are collectively represented as a turbulence source and a momentum sink within the vertical levels containing the turbine rotor disc [9].

Fitch's parameterization is implemented within the Mellor-Yamada-Nakanishi-Niino (MYNN) 2.5 boundary layer scheme [12], where the wind-farm effects are parameterized on the Reynolds averaged Navier-Stokes (RANS) flow. In the MYNN model the effects of buoyancy on pressure covariances and stability on the mixing length scale are included. This model determines the empirical closure constants from LES database for a dry atmosphere, what makes the TKE forecast more reliable.

In the WFP the rate of change of kinetic energy within a grid cell is equated to the rate of kinetic energy extracted by the virtual WTs in that cell, from which a fraction is converted to power, and the rest contributes to turbulence generation. All these magnitudes, derived from the drag force induced by a WT, such as momentum-tendency, TKE source and power converted into useful electrical energy (equations 1, 2 and 3, respectively), are computed in terms of the horizontal wind speed modulus in the cell, $|V|_{ijk}$:

$$\frac{\partial |\mathbf{V}|_{ijk}}{\partial t} = -\frac{\frac{1}{2} N_t^{ij} C_T(|\mathbf{V}|_{ijk}) |\mathbf{V}|_{ijk}^2 A_{ijk}}{(z_{k+1} - z_k)}, \tag{1}$$

$$\frac{\partial TKE_{ijk}}{\partial t} = \frac{\frac{1}{2} N_t^{ij} C_{TKE}(|\mathbf{V}|_{ijk}) |\mathbf{V}|_{ijk}^3 A_{ijk}}{(z_{k+1} - z_k)}, \tag{2}$$

$$P_{ijk} = \frac{1}{2} N_t^{ij} \Delta x \Delta y C_P(|\mathbf{V}|_{ijk}) \rho_{ijk} |\mathbf{V}|_{ijk}^3 A_{ijk}, \tag{3}$$

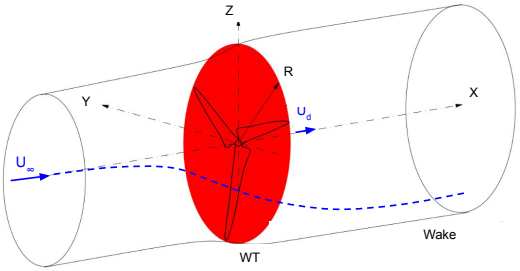

Figure 1. Actuator disc model: Speed field around the disc location (red).

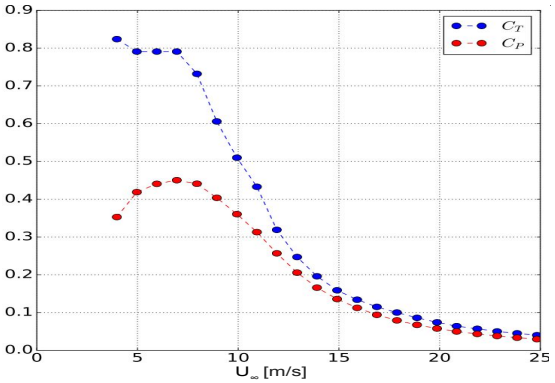

Figure 2. Vestas V90: Thrust and power coefficients provided by the manufacturer.

where N_t^{ij} is the number of wind turbines in the grid cell, ρ_{ijk} is the air density and A_{ijk} is the cross-sectional rotor area of one wind turbine bounded by model levels $k, k+1$. C_T and C_P are the thrust and power coefficients, which are also function of $|V|_{ijk}$ and $C_{TKE} = C_T - C_P$ according the assumption that the part of the kinetic energy not directly converted into power is turn into turbulence.

2.2. Induction-Aware Wind Farm Parameterization (IAWFP)

In the standard actuator disc (AD) model [13, 14], the force exerted by a WT on the flow is uniformly distributed on the disc area, represented in red in Figure 1. It depends on the undisturbed velocity U_∞ at hub height far upstream of the disc and the thrust coefficient C_T, which in turn also depends on U_∞ (Figure 2). Due to the turbine induction, U_∞ is reduced at the disc location and further on downwind. In the present work this idea is reconsidered and the WFP is modified to make it aware of the induction zone produced by the parameterized WTs (this modified parameterization is refereed hereon as IAWFP). This is achieved by working with a "reference velocity", U_∞, instead of the speed in the grid cell that contains the WT, $|V|_{ijk}$. Thus, both the coefficients and the equations 1 to 3 are computed in terms of this reference velocity.

In order to relate the undisturbed or reference velocity, U_∞, with the local WT grid cell velocity, $|V|_{ijk}$, a calibration process was devised, similar to the one performed in [14]. In this procedure, a single WT is simulated in the WRF model imposing a thrust corresponding to the selected undisturbed velocity, and according to the WT specifications. A first modified version of the WFP was produced with this goal, in which the exact thrust is applied to the grid cell which contains the turbine. The WRF was then compiled for an idealized case with flat terrain and a fixed roughness length, including the Coriolis forcing and disregarding heat fluxes from the surface.

The simulations are initialized with a constant geostrophic wind, imposed in agreement with the targeted velocity, and a slightly stable atmosphere. The model configuration and targeted velocities are summarized in Table 1. After a 4-day spin-up simulation, the wind converged to a logarithmic neutral profile with the targeted velocity at hub height. Once the initial field is achieved, a 1-day long simulation is performed placing a wind turbine in the center of the domain, activating the modified WFP which imposes the exact thrust that corresponds to the undisturbed velocity. This procedure is repeated for different velocities (see Table 1) and several horizontal resolutions.

Table 1. Model configuration.

Domain size in x, y (km):	20 x 20
Vertical levels:	40, with 15 levels under 200 m
Roughness length:	0.01 m
Coriolis frequency (s^{-1}):	-1 x 10^{-4}
Boundary conditions:	Open
PBL scheme:	MYNN 2.5 [12]
Surface layer scheme:	MM5 Monin–Obukhov scheme [15]
U_∞ simulated (m/s):	6, 8, 10 and 12

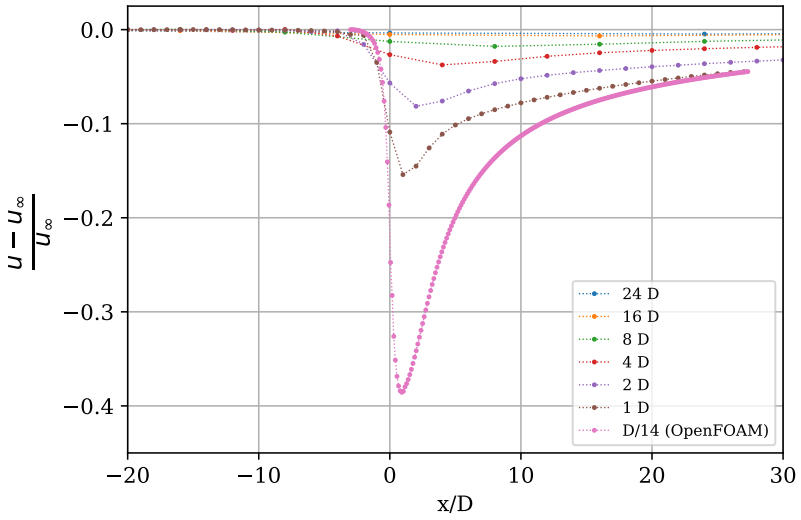

Figure 3. Wind speed deficit along the wind direction for different horizontal resolutions.

As an example of the resulting behavior of of the flow, Figure 3 shows the axial wind speed deficit for the 8 m/s undisturbed velocity with the total thrust applied consistently. The speed deficit varies with the resolution, given that the momentum sink is distributed over larger cells as the resolution is decreased resulting in a smaller impact. It is clear that the grid cell velocity (at 0D) strongly depends on the chosen resolution which is thus made explicit in the U_∞ vs $|V|_{ijk}$ relation. This way the model induction from the WFP inside WRF is captured.

In order to get an approximation to the actual velocity field in the vicinity of a wind turbine to compare with the WRF results, figure 3 includes the outcome of a high definition stationary simulation of the flow. A flow solution that was obtained using the AD model [14] to represent the wind turbine in OpenFOAM, with horizontal resolutions of $D/14$ in the surroundings of the wind turbines and $D/7$ in the rest of the domain to more precisely represent the phenomena. This methodology was already validated, among other situations, for neutral ABL conditions in the wind farm taken as study case in section 3.2 [14]. In order to make results from both sources as comparable as possible, given that both the WFP and the boundary layer parameterization on which it depends are based on a RANS approach, a stationary RANS simulation was conducted. The Realizable k-ϵ with standard coefficients was used as turbulence closure model. The initial and boundary conditions were set to produce compatible conditions to those of the WRF, a neutral logarithmic wind profile with 8 m/s at hub height and the same roughness length. On the other hand, we let WRF simulations to stabilize in order to attain stationary solutions. One difference between both approaches is the way turbulence is incorporated. While in the

OpenFOAM approach turbulence is not explicitly added by the model, but generated due to shear stresses originated in the volumetric forces induced by the AD model, the WFP has an explicit TKE source term which injects turbulence into the flow, and this could be the major difference between both approaches as this turbulence will certainly have an effect on how wakes mix and dissipate. Although not directly comparable, these results provide complementary insight into the interaction process, and the RANS simulation with AD can be considered as a high resolution limiting case. As it can be seen in Figure 3, when the resolution is increased in the WRF model the results tend to those obtained with much higher resolutions from OpenFOAM.

Summing up, a single wind turbine is simulated for a wide range of known U_∞ and different grid sizes, imposing the respective thrust, and registering the resulting velocity on the WT cell. This calibration process yields the induction-aware relation for $|V|_{ijk}$ as a function of U_∞ and the resolution. Thus, the WFP is modified in order to account for this relation making equations 1 to 3 and the respective coefficients depend on U_∞, obtaining the IAWFP implementation in WRF.

3. Results

3.1. Verification of the IAWFP with one single wind turbine

As a means of verification, single wind turbine simulations were performed with the objective of corroborating that the IAWFP was effectively not affected by resolution changes. WRF with the IAWFP was configured as described in Table 1 selecting different horizontal resolutions from those performed in the calibration process. Resolutions of 2000 m, 1000 m, 500 m and 250 m were used in these simulations. Results were contrasted with those of other two parameterizations run with the same model configuration: the standard WFP, and the EWP [16], another parameterization frequently used and implemented in WRF, for which an initial length scale factor, σ_0, equal to 1.7 is adopted.

Figure 4 shows the power production of a single Vestas V90 turbine (C_T and C_P in Figure 2) obtained from the three parameterizations with different horizontal resolutions and for three reference wind speeds. This magnitude is presented as indicator, being the one typically outputted by the parameterizations. Nonetheless, the same behavior is also observed for the momentum sink and the TKE source, which are not directly exposed but computed based on similar equations. It can be observed, that the only parameterization that consistently computes the power according to the imposed velocity and independently of the resolution is the IAWFP.

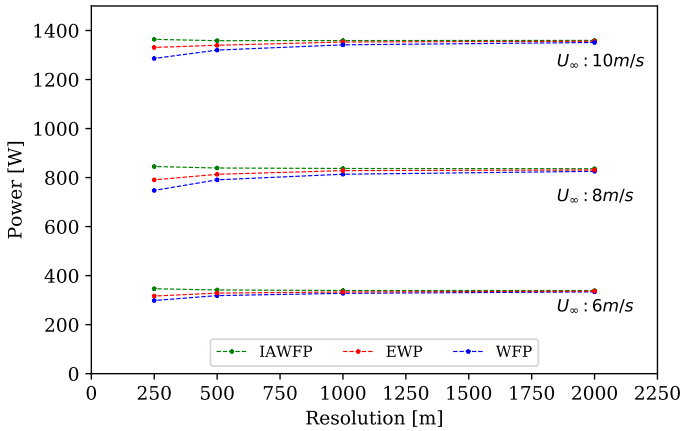

Figure 4. Power predicted for a single WT with different horizontal resolutions.

The effect of the parameterizations on the wind flow is shown in Figure 5 for different grid resolutions. As expected, the speed deficit at the hub height depends on the resolution. This makes sense since the momentum sink as the resolution decreases, is distributed over a greater area and therefore represents a smaller impact. However, it can be seen that the EWP produces around half the speed deficit that the WFP and IAWFP which would result in a weaker wake. On the other hand, the deficit looks quite similar for the WFP and the IAWFP, but as seen in Figure 4, the small difference between them and the way power, thrust and TKE are computed produce significant differences in those aggregated magnitudes. In order to confirm that the premises of the new parameterization hold, the IAWFP was implemented with the capacity of outputting the total thrust applied at each grid cell. When evaluating its value, it is verified that it remains constant for all resolutions, showing that the total thrust is now only related to U_∞ and is therefore independent of the resolution chosen. The other two parameterizations could not be compared in this sense, since they do not output the applied thrust.

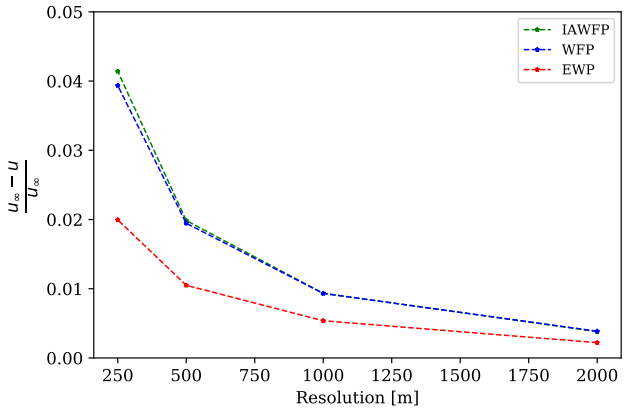

Figure 5. Wind speed deficit at hub height for a single WT with different horizontal resolutions. Undisturbed wind speed $U_\infty \approx 8$ m/s.

3.2. Power estimation for different directions

In this section the IAWFP is applied to the simulation of an idealized version of an actual utility-scale wind farm in order to explore its capacities to represent the wakes. The Rawson wind farm (RWF) is located in Patagonia, Argentina. It is placed on not complex terrain, 10 km far from the sea coast, at 43° S latitude. In the first two development stages the RWF had 43 Vesta V90 wind turbines, with 80 m hub height, 90 m diameter (D) and 1.8 MW of nominal power. These turbines are arranged in 4 rows with north-west south-east orientation, $12D$ of separation between rows and $4D$ between wind turbines in a row, resulting in an area of around 4.5 km $\times$ 4.5 km (Figure 6). For the idealized version it is assumed that the RWF is placed on flat terrain with a 0.01 m roughness length.

Even though each wind farm has a defined layout, wind farm parameterizations, given a grid size, re-arrange them placing one or more wind turbines in the center of the corresponding grid cell according to their position. Figure 6 shows how the WFP re-arrange or interpret the RWF layout for three different horizontal resolutions. It is clear that the real farm layout is misrepresented for coarser resolutions, left and central panels, masking the directional dependency of the wind farm effect. The most unfavorable direction is not distinguished with these resolutions. Moreover, for 1 km grid size (left panel), too many wind turbines are placed on the same cell. This high WT density in a grid tends to overestimate the wind power produced in

the cell as the interference between them is not contemplated by none these parameterization. This shows the possible improvement that would be achieved working with resolutions that correctly describe the distribution of the wind turbines in the park.

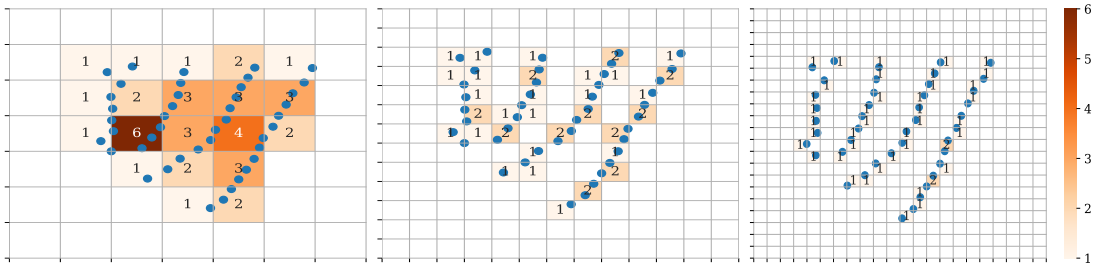

Figure 6. Rawson wind farm layout (blue dots). How the parameterization re-arrange the layout according to three horizontal resolutions, 1km (left), 500 m (center), 300 m (right). Number of wind turbines per grid cell in oranges.

There are several works in which the WFP is used with high resolution grids, even reaching the frontier between mesoscale and LES (around 300 m), the so-called terra incognita [17]. In [18], where the performance of the WFP is evaluated for different vertical and horizontal resolutions, reaching horizontal resolutions of 500 m, it is concluded that finer resolutions have great impacts on the simulated wake flow dynamics. Moreover, both in [19] and [20], WFP is used for high resolutions (333m) for onshore and offshore wind farms, respectively. The importance of performing WRF high-resolution simulation is highlighted in both cases. Furthermore, the effects of representing a wind-turbine array using the AD in LES and RANS in WRF are analyzed in [21]. Despite finding an overestimation of TKE generation in the WFP, it is conclude that it can qualitatively replicate the majority of wind speed and TKE impacts of a LES simulation. In this work, the wind farm parameterizations performance is explored for different horizontal resolutions, for grid sizes ranging from one kilometer to 300 m.

The RWF efficiency for all wind directions, computed every 11.25°, and several resolutions is presented in Figure 7. The power production of the wind farm is normalized by the expected production of 43 times a single wind turbine to calculate the park efficiency. These idealized simulations were conducted following Table 1 configuration but only for $U_\infty = 8$ m/s (the mean wind speed for the farm location), using the three wind farm parameterizations: EWP, WFP and IAWFP, and three horizontal resolutions: 1 km, 500 m and 300 m. Again the neutral wind profiles and the desired winds at hub height are achieved after 4-day spin-up simulations initializing with a specific constant geostrophic wind and a slightly stable atmosphere. As these are idealized neutral condition simulations with no terrain, the power measurements at RFW cannot be used to validate, therefore results obtained from OpenFOAM simulations, working with 7 m resolution, regarded as close to the "actual" behavior of the park, are also shown in Figure 7 for comparison. The results reveal a clear reduction of the power production for wind directions of 22.5° and 202.5°. The higher power deficit at these directions is a consequence of the wind farm layout, since these directions almost coincide with the farm rows orientation. These less favorable directions are detected by the three parameterizations, but only when they are made to work with the highest simulated spatial resolution, 300 m. This is clearly explained by Figure 6, where the layout of the park is almost perfectly represented under this resolution and therefore the minimum efficiency directions are exposed. However, it can be observed that when the resolution is increased, both the WFP and the EWP, tend to report lower mean farm efficiency, although in the case of the EWP this behavior is not as strong, may be due to the

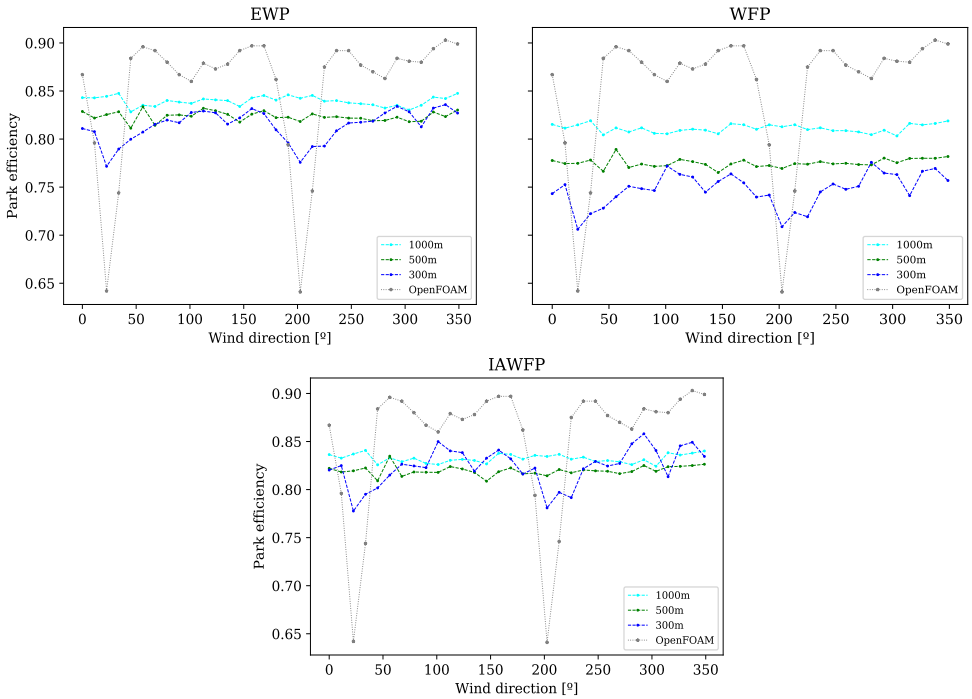

Figure 7. Rawson wind farm efficiency versus wind direction at 8 m/s. Simulation results from the EWP (top left), WFP (top right) and the IAWFP (bottom).

way power is computed in this parameterization. The only one of the three parameterizations that shows independence with respect to the resolution is the IAWFP, behavior also evidenced in section 3.1.

Regarding the IAWFP, Figure 7 (bottom) shows it to be the least sensitive to the selected resolution. Also it can be observed that when the resolution is increased the effect of the wind farm layout is better captured and therefore, the directions for which the efficiency of the park reaches extreme values become more evident and closer to what is seen in OpenFOAM results. Near the maximum interference directions, where the minimums are attained, averaging the momentum sink in cells 3 times larger than the rotor disc softens this effect and spreads it in a wider range of directions.

Figure 8 shows a comparison of the wakes produced by the IAWFP at 1 km and 300 m resolutions for two representative wind speeds: 270° the main direction at the farm location and 22.5° the direction with the higher interference according to the farm layout. It is clear that the wind farm wakes are described with more detail at high resolutions for both wind directions. The 1 km resolution produces almost the same wake effect in the two directions, while with 300 m more details of the wake are revealed. Thus, the 22.5° wind direction produces a deeper wake effect than 270° with high deficit due to the turbines being almost perfectly aligned.

4. Conclusion, discussion and further work

With wind turbines growing in height and wind farms covering an ever broader surface area, a better representation of how turbines and farms interact with the lower layers of the atmosphere and vice versa becomes necessary. This need lies in the importance of correctly characterize the impact of wind farms in mesoscale numerical weather prediction models that allow to simulate long periods of time at not-so-high computational costs. In this sense, a new wind farm parameterization was developed and implemented in WRF. The IAWFP relates the undisturbed

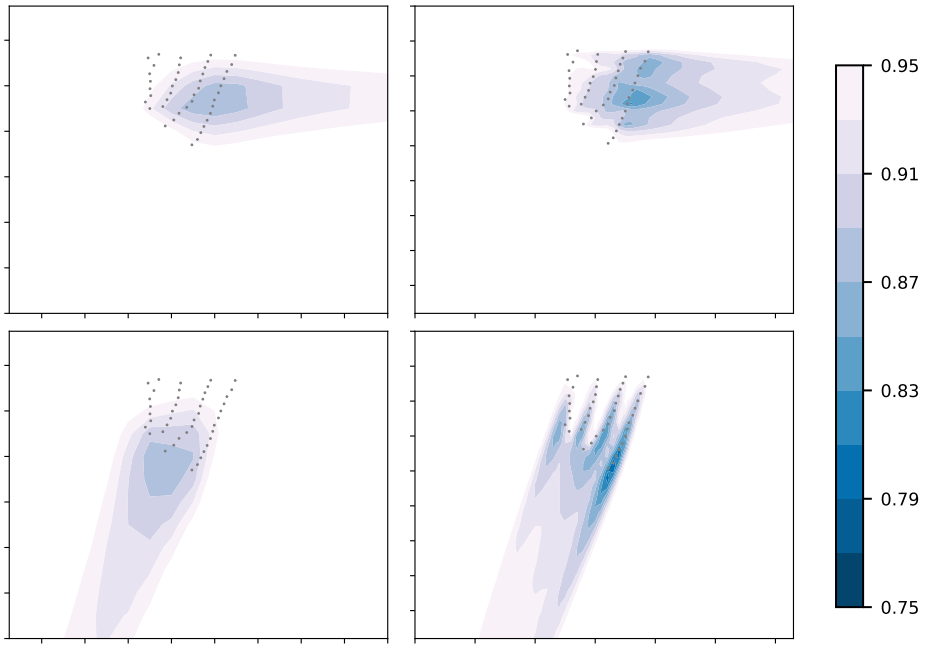

Figure 8. Rawson wind speed deficit ($\frac{U}{U_\infty}$) at hub height, simulated with the IAWFP for two wind directions, 270° (top), 22.5° (bottom) and two horizontal resolutions, 1 km (left), 300 m (right). $U_\infty = 8$ m/s.

wind speed several diameters upstream of the turbine, with the wind speed in the cell that contains the turbine. This U_∞ is then used to compute the drag forces exerted on the flow, the power production and the increase in TKE due to the turbines.

In the aim of performing a verification of the IAWFP, single wind turbine simulations have been compared with those from other classical parameterizations, the WFP and the EWP, showing mainly that the predicted power output is well computed and independent of the grid cell size in the IAWFP. Once the new wind farm parameterization was checked for a single turbine, it was used, together with the previous ones, to simulate an idealized case of the Rawson wind farm. The main and conclusive results of these simulations were that the IAWFP showed to be insensible to the grid resolution, in terms of mean efficiency, and therefore related exclusively with the reference speed, U_∞. But they also revealed the need of performing simulations at high resolutions in order to capture the effect of the actual wind farm layout and consequently detect the wind directions of greater and lesser efficiency. It should also be mentioned that averaging due to grid cells much larger than the rotor disc smooth out this effect and spread the interference over a wider range of directions, which explain the differences with the higher resolution OpenFOAM results for directions of great interference. This last effect and the inability of this kind of parameterizations to account for the intracell interference among turbines are the main drawbacks of this approach. The latter issue is partially solved moving towards higher resolutions which is only viable with the IAWFP.

It is important to mention that both in [9] and in [22], it is stated that the WFP represents the far-wake (greater than 5 rotor diameters, following [23]), and therefore it is recommended to apply it for resolutions greater than this distance. The reason for that is two-fold:

(i) It was argued that for higher horizontal resolutions the wake rotation should be considered in the model [9].

(ii) For the standard commercial wind turbines at the time the WFP was developed, that

resolution was very near to the mesoscale–LES limit mentioned above.

The first recommendation is based on the fact that some authors have found a differentiation between the near and far wake, using more precise techniques and higher resolutions. This difference appears when complex phenomena, like non-uniform distribution of the thrust and rotational forces, are included in more descriptive approaches such as CFD simulations combined with the AD model. Nonetheless, [23] and [24] have shown that the inclusion of these phenomena generates differences in the resolved wake only for distances closer than $5D$. According to [24], this distance is reduced to 2.5D when the WT works for wind speeds below the rated value. Despite these minor differences in the near wake, many authors [25, 14, 26] agree that the inclusion of these details has a small influence on the flow behavior. This is even more true in the case of parameterizations working in a greater scale. Regarding this, in this work the possibility to explore the performance of the new parameterization for resolutions close to the near wake was carried out, but respecting the mesoscale–LES limit. Thus, higher resolutions allow to capture more details in the farm wake and interaction with the lower layers flow. The promising results observed adapting Fitch's parameterization implemented in the MYNN2.5 PBL scheme, encourage us to try to move forward to more sophisticated PBL schemes more appropiated for higher resolutions.

Future work will attempt to improve the way the IAWFP estimate the source of TKE produced by wind turbine rotating blades. It has been featured in [27], [10] and [21] that the standard wind farm parameterization tends to overestimate the TKE source. In [28] it is also noticed that the WFP adds too much TKE at the upwind side of a wind farm. Therefore, future research will focus on enhance this feature based on, for example, the work of [10].

5. Acknowledgments

This work was supported by the National Scientific and Technical Research Council [grant PIP 11220120100480CO]; the National Agency for Scientific and Technological Promotion [grant PICT2013-1338]. The RWF specifications were kindly provided by GENNEIA S.A. The authors acknowledge the computational made available by the CSC-CONICET.

References

[1] Kirk-Davidoff D B and Keith D W 2008 *Journal of the Atmospheric Sciences* **65** 2215–2234
[2] Wang C and Prinn R G 2010 *Atmospheric Chemistry and Physics* **10** 2053–2061
[3] Fitch A C, Olson J B and Lundquist J K 2013 *Journal of Climate* **26** 6439–6458
[4] Calaf M, Parlange M B and Meneveau C 2011 *Physics of Fluids* **23** 126603
[5] Joulin P A, Mayol M L, Masson V, Blondel F, Rodier Q, Cathelain M and Lac C 2019 *Frontiers in Earth Science* **7** 350
[6] Churchfield M, Lee S, Moriarty P, Martinez L, Leonardi S, Vijayakumar G and Brasseur J 2012 A large-eddy simulation of wind-plant aerodynamics *50th AIAA Aerospace Sciences Meeting including the New Horizons Forum and Aerospace Exposition* p 537
[7] Baidya Roy S, Pacala S and Walko R 2004 *Journal of Geophysical Research: Atmospheres* **109** D19
[8] Blahak U, Goretzki B and Meis J 2010 A simple parameterization of drag forces induced by large wind farms for numerical weather prediction models *Proceedings of the European Wind Energy Conference & Exhibition* vol 1 pp 4577–4585
[9] Fitch A, Olson J, Lundquist J, Dudhia J, Gupta A, Michalakes J and Barstad I 2012 *Monthly Weather Review* **140** 3017–3038
[10] Abkar M and Porté-Agel F 2015 *Journal of Renewable and Sustainable Energy* **7** 013121
[11] Skamarock W, Klemp J, Dudhia J, Gill D, Barker D M, Wang W and Powers J 2008 A description of the advanced research WRF version 3 Technical note NCAR/TN-475+STR University Corporation for Atmospheric Research doi:10.5065/D68S4MVH
[12] Nakanishi M and Niino H 2009 *Journal of the Meteorological Society of Japan. Ser. II* **87** 895–912
[13] Burton T, Sharpe D and Jenkins N 2001 *Handbook of wind energy* (John Wiley & Sons)
[14] Navarro Diaz G P, Saulo A C and Otero A D 2019 *Journal of Wind Engineering and Industrial Aerodynamics* **186** 58–67

[15] Chen F and Dudhia J 2001 *Monthly Weather Review* **129** 587–604
[16] Volker P, Badger J, Hahmann A and Ott S 2015 *Geoscientific Model Development Discussions* **8** 3481–3522
[17] Wyngaard J C 2004 *Journal of the atmospheric sciences* **61** 1816–1826
[18] Mangara R J, Guo Z and Li S 2019 *Advances in Atmospheric Sciences* **36** 119–132
[19] Prósper M A, Otero-Casal C, Fernández F C and Miguez-Macho G 2019 *Renewable energy* **135** 674–686
[20] Jiménez P A, Navarro J, Palomares A M and Dudhia J 2015 *Wind Energy* **18** 559–566
[21] Vanderwende B J, Kosović B, Lundquist J K and Mirocha J D 2016 *Journal of Advances in Modeling Earth Systems* **8** 1376–1390
[22] Fitch A C 2016 *Wind Energy* **19** 1757–1758
[23] Wu Y T and Porté-Agel F 2011 *Boundary-layer meteorology* **138** 345–366
[24] Navarro Diaz G P, Saulo A C and Otero A D 2019 Comparative study on the wake description using actuator disc model with increasing level of complexity *Journal of Physics: Conference Series* vol 1256 (IOP Publishing) p 012017
[25] van der Laan M P, Sørensen N N, Réthoré P E, Mann J, Kelly M C and Troldborg N 2015 *Wind Energy* **18** 2223–2240
[26] Castellani F and Vignaroli A 2013 *Applied Energy* **101** 432–440
[27] Eriksson O, Lindvall J, Breton S P and Ivanell S 2015 Wake downstream of the lillgrund wind farm. a comparison between LES using the actuator disc method and a wind farm parametrization in WRF *Journal of physics: Conference series* vol 625 (IOP Publishing) p 012028
[28] Siedersleben S K, Platis A, Lundquist J K, Djath B, Lampert A, Bärfuss K, Cañadillas B, Schulz-Stellenfleth J, Bange J, Neumann T and Emeis S 2020 *Geoscientific Model Development* **13** 249–268